The Cryosphere Discuss., 5, 1311–1334, 2011
www.the-cryosphere-discuss.net/5/1311/2011/
doi:10.5194/tcd-5-1311-2011

The Cryosphere Discussions

Recent wind driven high sea ice export in the Fram Strait contributes to Arctic sea ice decline

L. H. Smedsrud[1], **A. Sirevaag** [2,1], **K. Kloster**[3], **A. Sorteberg**[2,1], **and S. Sandven**[3]

[1]Bjerknes Center for Climate Research, Bergen, Norway
[2]Geophysical Institute, Univ. of Bergen, Norway
[3]Nansen Environmental and Remote Sensing Centre, Bergen, Norway

Received: 5 April 2011 – Accepted: 18 April 2011 – Published: 5 May 2011

Correspondence to: L. H. Smedsrud (lars.smedsrud@uni.no)

Published by Copernicus Publications on behalf of the European Geosciences Union.

Abstract

Arctic sea ice area decrease has been visible for two decades, and continues at a steady rate. Apart from melting, the southward drift through Fram Strait is the main loss. We present high resolution sea ice drift across 79° N from 2004 to 2010. The ice drift is based on radar satellite data and correspond well with variability in local geostrophic wind. The underlying current contributes with a constant southward speed close to 5 cm s^{-1}, and drives about 33 % of the ice export. We use geostrophic winds derived from reanalysis data to calculate the Fram Strait ice area export back to 1957, finding that the sea ice area export recently is about 25 % larger than during the 1960's. The increase in ice export occurred mostly during winter and is directly connected to higher southward ice drift velocities, due to stronger geostrophic winds. The increase in ice drift is large enough to counteract a decrease in ice concentration of the exported sea ice. Using storm tracking we link changes in geostrophic winds to more intense Nordic Sea low pressure systems. Annual sea ice export likely has a significant influence on the summer sea ice variability and we find low values in the 60's, the late 80's and 90's, and particularly high values during 2005–2008. The study highlight the possible role of variability in ice export as an explanatory factor for understanding the dramatic loss of Arctic sea ice the last decades.

1 Introduction

Arctic sea ice area has decreased since the 1990's (Gloersen and Campbell, 1991). Regardless of the definition of the summer minimum sea ice area (average sea ice extent for September, minimum of daily sea ice area, or the local temporal minimum), the trend is now close to −9 % per decade (Zwally and Gloersen, 2008). Much discussion arose after the minimum September ice cover in 2007 (Stroeve et al., 2007), but the ice area loss has been back on a linear trend recently (Stroeve and Meier, 2010). These linear trends suggest a summer ice free Arctic between 2050 and 2080, comparable

TCD
5, 1311–1334, 2011

to 1-D models applying increased long wave radiation due to ongoing global warming (Smedsrud et al., 2008). Less predictable future changes are related to changes in cloud cover (Sorteberg et al., 2007) and atmospheric circulation (Overland et al., 2008).

For better predictions of future Arctic sea ice evolution we need to understand past changes. The present generation of General Circulation Models generally underestimates the ice loss during the last decades (Stroeve et al., 2007), and future predictions indicate a range from steady state year 2000 conditions, to no summer ice in 2080 (Boe et al., 2009). The Arctic sea ice cover responds to many different types of forcing, but the ice export clearly has direct impact (Björk, 1997), and may have contributed effectively to the observed sea ice thinning (Haas et al. 2008; Kwok, 2009). An increase in the ice export leads to more open water, more solar radiation into the ocean mixed layer, and stronger summer melting (Perovich et al., 2008). The decreasing ice and snow cover has also produced the near-surface temperature 'amplification' and increasing incoming long-wave radiation due to increased moisture fluxes (Screen and Simmonds, 2010), both positive feedback mechanisms.

The destiny of many Arctic sea ice floes is to leave the Arctic Ocean along the eastern coast of Greenland (Fig. 1). As first documented by the passive drift of the ship Fram (Nansen, 1906), a large area of sea ice is lost annually from the Arctic Ocean to the Greenland Sea through what was later termed the Fram Strait. Around 10 % of the Arctic sea ice cover is exported annually, and estimates have improved over the last decade (Vinje, 2001; Kwok et al., 2004; Kwok, 2009).

Trends in Fram Strait sea ice export have previously not been found, but within the Arctic Ocean sea ice drift speed has increased based on ice station and bouy data since the 1950's (Hakkinen et al., 2008). Increased speed has also been detected in the Fram Strait after 1979. Section 3 presents southward ice velocities across 79° N in the Fram strait based on high accuracy Synthetic Aperture Radar (SAR) data onwards from 2004. High correlations between the ice drift and geostrophic winds from atmospheric reanalysis data allow for calculations of the sea ice export back to the 1950's.

TCD
5, 1311–1334, 2011

Earlier estimates of sea ice export and speed have mostly been based on passive satellite data with coarser spatial resolution (Rampal et al. 2009; Kwok, 2009). We find that the ice export has been high in recent years, and discuss likely consequences and causes of this high export in Sect. 4. We conclude (Sect. 5) that the recent high ice export must have influenced both the September minimum ice cover of the last few years, and the general thinning of Arctic sea ice.

2 Data and methods

Sea ice area export was calculated from sea ice motion and ice concentration profiles along 79° N. Onwards from August 2004 ice drift vectors were calculated from pairs of Envisat ASAR WideSwath images captured 3 days apart with uninterrupted year-round coverage. Images were averaged to 300 m/pixel spatial resolution, corresponding to a speckle noise well below 0.3 dB.

The manually recognized persistent ice features were gridded to 2 km accuracy and the corresponding displacement vectors that cross 79N were linearly interpolated to bins (1° longitude, each 21 km) from 15° W to 5° E. For most 3-day image pairs, displacement vectors with accuracy about 10 % were found with a spacing of 30–50 km, including interpolation/extrapolation in the shear/ice edge zones. As the vectors can be assumed non-biased, cumulative motion over longer periods will have improved accuracy. We based ice concentration on Norsex algorithms used respectively on DMSP F13 SSMI and AQUA AMSR–E brightness temperature data, giving the combined ice-area flux along 79° N, between 2004 and 2010 (Kloster and Sandven, 2011). Our mean of approx. 4500 observations of sea ice velocity along 79° N was 12.0 cm s^{-1} southward (s.d. ± 8.7) with a small westward component (4.3 cm s^{-1}, s.d. ± 5.7). Monthly mean area export uncertainties were estimated to 5 %.

We used sea level pressure difference from 80° N in the NCEP/NCAR reanalysis products (Kalnay et al., 1996) from 1957-present. As air pressure measurements were not synchronised globally before the International Geophysical Year in 1957 we have

TCD
5, 1311–1334, 2011

omitted the 1948–57 period. Pressure difference (ΔP) from 25° W and 5° E was extracted (Fig. 1), and used to estimate correlations and linear regression estimates between geostrophic wind (V_g) and sea ice drift speed (V_{ice}) or ice area export (F_{ice}).

Estimation of confidence levels takes into account serial correlation in the datasets by using the effective number of observations instead of the sample size in the significance estimate (Quenouille, 1952; Sorteberg and Kvingedal, 2006). Number of independent observations was typically reduced by ∼50 % using this procedure.

An algorithm for feature tracking developed by Hodges (1994) and Hodges (1999) was used to construct storm tracks from the 6 hourly NCEP/NCAR reanalysis data from 1957 to 2007. The dataset is an updated version of the one used in Sorteberg and Walsh (2008) where 850 hPa relative vorticity was used to identify the cyclones. To remove the influence of the the background flow (pressure in cyclones moving northward tends to drop faster than a system moving southward due to the ambient pressure being lower at northern latitudes) the large scale flow was filtered out (Anderson et al., 2003) before the synoptic low pressures were identified. For details see Sorteberg et al. (2007).

3 Results

Sea ice drift in general is created largely by the wind above, and the ocean current below the sea ice (Thorndike and Colony, 1982). The short-term variability is usually mostly wind driven, and this is also the case for Fram Strait ice speed and the related sea ice export (Vinje, 2001; Widell et al., 2003; Kwok et al., 2004; Tsukernik et al., 2009). In addition the Fram Strait ice export is guided by the nearby Greenland coast, and rides on the underlying East Greenland Current.

TCD
5, 1311–1334, 2011

3.1 Relationship between ice export and local wind

Figure 2 shows our linear fit for geostrophic wind and ice velocity (Eq. 1). The Fram Strait average ice velocity is 1.4 % of the geostrophic wind speed. The linear regression between ΔP and V_{ice} (1) gave coefficients comparable to classical values (Thorndike and Colony, 1982).

$$V_{\text{ice}} = 0.014 \times V_{\text{g}} + 0.050 \quad [\text{ms}^{-1}] \tag{1}$$

where

$$V_{\text{g}} = (1/f\rho_a) \times (\Delta P/\Delta x) \quad [\text{ms}^{-1}]. \tag{2}$$

Here $f = 2\Omega\sin(80) = 1.43610^{-4}\,\text{s}^{-1}$, the Coriolis parameter, $\rho_a = 1.3\,\text{kg}\,\text{m}^{-3}$, the density of air, and $\Delta x = 573\,\text{km}$, the distance over the ΔP from 25° W to 5° E on 80° N. The correlation for the NCEP based V_{ice} (Eq. (1) and the observed V_{ice} was good ($r_{\text{speed}} = 0.83[0.74 - 0.90]$). Figure 2 shows the linear regression and that monthly averages of the ice speed ranges between zero and $25\,\text{cm}\,\text{s}^{-1}$.

We found a similar relationship as Eq. 1 between ΔP and the ice area export:

$$F_{\text{ice}} = 8737\Delta P + 24562 \quad [\text{km/month}]. \tag{3}$$

Correlation between sea ice area export and pressure difference Eg. (3) was also good ($r_{\text{area}} = 0.80[0.68 - 0.87]$). A similar relationship between the pressure difference and sea ice area export was obtained using the ERA40 data and the correlation between NCEP and ERA40 (Uppala et al., 2005) reanalysis pressure difference was excellent ($r = 0.96$).

3.2 Ice export variability

Along 79° N ice area export is limited at both sides. In winter, the sea ice is stationary as fast ice westward of 16° W to 12° W (Fig. 1). A relatively narrow shear zone is

TCD
5, 1311–1334, 2011

found eastward, with a gradual increase in speed further east. On the whole western side ice concentration is close to 100 % during winter, but ice drift is low (Fig. 1). On the eastern end ice export is limited by zero concentration, varying between 5° W and 5° E. Ice velocity generally increases eastward, while sea ice concentration decreases, creating a peak in ice area export near 5° W (Figs. 1 and 6). The yearly cycle in area export is pronounced. Figure 3 shows that the major export occurs between October and April, and that there is close to zero export in July and August.

We found no evidence for a seasonal cycle in the East Greenland Current. Foldvik et al. (1988) analysed one year long time series from three moorings along 79° N between 6 and 2° W and found large mesoscale eddies meandering southwards, but no obvious seasonal variability. Southward flow was in the range 6.2 to 9.5 cm s^{-1}, decreasing east of 2° W. Our results with a mean southward flow throughout the year between 2004 and 2010 is thus consistent with earlier studies. From Eq. (1) the mean current is estimated to 4.95 cm s^{-1}, also consistent with current measurements from 79° N 5° W (Widell et al., 2003) between 1996 and 2000. Figure 4 shows that since 2004 the ice export approaches zero for two to three summer months every year. This is caused by winds from the south (negative cross straight pressure gradient) opposing the steady southwards flowing current below the sea ice.

In the case of no wind forcing, or zero cross straight pressure difference, there is still a steady export of sea ice. Our contribution from this steady current is an ice area flux of 24 562 km^2 pr month, This means that the East Greenland Current has driven ~33 % of the ice export since 2004. Compared to previous estimates at 81° N (Kwok, 2009) our pressure dependency is 19 % larger, while our constant term (Eq. 3) is 12 % lower. Ice speed correlates better with geostrophic wind than ice area export ($r_{speed} > r_{area}$), probably because geostrophic wind influences ice concentration to a small degree.

3.3 SAR – AMSR Comparison

We compared our SAR based ice speed data directly with ice speed estimates based on Advanced Multichannel Scanning Radiometer (AMSR) (Ezraty et al., 2010). AMSR

TCD
5, 1311–1334, 2011

data is available (from October through April), and we therefore used 3-day periods for this period of the year in our comparison. Generally no ice speed estimates are available from passive satellites during summer, but it is the winter months that have the largest ice area flux (Fig. 3). For each 3-day period from February 2004 to April 2010 available AMSR ice drift vectors crossing 79° N were averaged in the same longitude bins as for the SAR data. Figure 5 compares the northward velocity components for time periods and longitude intervals where velocity data exists in both data sets. AMSR data exist for overall 34 % of the total number of longitude bins. The linear fit in Fig. 5 shows that there is good correspondence in the mean between SAR and AMSR derived drift vectors. The considerable spread may be caused by several factors, but we hold these to be the most important: (1) the vectors time-of-day may differ, (2) AMSR has many non-zero drifts in the fast ice (at zero SAR speed), and (3) AMSR often under-estimates large speeds (at high SAR speed). However, on the average the figure gives a good reassurance in the two data sets, and indicates that the magnitude of the northward velocity estimates over the 6 years are close to reality.

Figure 6 shows the temporal coverage of the AMSR data in each longitude bin. The AMSR data has good coverage in the westernmost longitude bins, but it is dropping below 10 % east of 3° W. The relative contribution to the total ice area flux for each longitude bin, derived from the SAR ice drift velocities, is also included in Fig. 6. In the bins between 15 and 10° W AMSR coverage is above 50 %, but these bins carry a very small part of the ice export. The average AMSR coverage in the longitude bins which accounted for more than 90 % of the total ice area flux (Fig. 6, 11 to 0° W), was as low as 29 %. The low temporal coverage of AMSR data in the longitude range which house most of the ice export during the winter season, is a likely explanation for why the variability demonstrated by our SAR based ice area fluxes have not been detected in other data sets.

TCD
5, 1311–1334, 2011

4 Discussion

4.1 Mean export and variability

Figure 4 shows that our pressure based estimate of monthly ice export (Eq. 3) captures the observations in a good way. The mean yearly ice export based on the SAR velocities since 2004 is 0.888 mill km^2, while the similar NCEP based value (Eq. 3) is 0.894 mill km^2. The largest bias is found during large export events in the winter time (Fig. 4), but the bias is generally lower than ∼10 %. The large export events during winter are usually caused by a combination of high ice speed (above 30 cm s^{-1}), and high ice concentrations. Using the full 50 years time series, our annual mean value is 0.771 mill km^2, clearly reflecting high values in recent years. This long term average is ∼10 % higher than the 1979–2007 value from Kwok (2009).

4.2 Long term trends

We find a decrease in ice concentration across 79° N of −1.3 % per decade, consistent with a similar decrease observed by Kwok (2009). The decrease in ice concentration since 1979 balanced increasing ice speed also observed by Kwok (2009), leading to no trend in ice export in that data set. In our data set the sensitivity towards the increasing pressure gradient is higher, and we therefore also get a larger increase in ice speed. The increasing southward ice drift velocity is large enough to create an increase in ice area flux. Annual mean velocity has increased from 10 to 12 cm s^{-1} since 1957. Our results are thus consistent with increasing 1979–2004 winter mean speed from passive micro-wave sensors (Rampal et al., 2009), and increasing ice drift speed within the Arctic Ocean (Hakkinen et al., 2008).

Figure 7 shows that the increasing ice speed creates a clear positive trend in sea ice area export over the last 50 years. After 2004 all years had an ice export larger than the long term average of 0.771 mill km^2. Trends are close to the overall 5 % increase per decade throughout the period, and no particular shift can be seen, but

TCD
5, 1311–1334, 2011

there are large year to year fluctuations. The cross-strait pressure difference trend is seasonally strongest during winter, weaker during autumn and spring, and close to zero during summer, consistent with earlier results (Hakkinen et al., 2008; Kwok, 2009). This makes the seasonal increase in ice export strongest during winter, smaller during spring and autumn, and practically zero during summer (Fig. 3). As a test of the sensitivity of the trend estimate to the choice of reanalysis we redid the calculations using the ERA40 reanalysis (Uppala et al., 2005) for the 1957–2003 period. A similar, but slightly weaker trend (13 % smaller) was found. Confirming that the trend estimates is not overly sensitive to the choice of reanalysis product.

The positive trend in sea ice export since 1957 (Fig. 7) is produced by a trend in the local pressure gradient (Eq. 3). The trend could be produced both by an increase in pressure on the Greenland (west) side, or a decrease on the Svalbard (east) side. We found that most of the trend is created by lower pressure in the east, and therefore searched for changes in the low pressure systems entering the region from the south-west. The cross straight trend is consistent with a sinking trend in sea level pressure in the Svalbard area in general as noted by Vinje (2001), and confirmed by updated sea level pressure data from Longyearbyen, Svalbard (not shown). Using the cyclone track data set (Sorteberg and Walsh, 2008) we found a link between the wintertime local pressure gradient trend and the intensification of cyclones over the Nordic Seas (intensity measure was relative vorticity in 850 hPa). The correlation between the local winter pressure difference and the intensity of the Nordic Seas (60–85° N and 20° W–30° E) cyclones ($r_{\text{cyclone}} = 0.75$) indicates that the local pressure difference is strongly related to cyclonic activity in the Nordic Seas. In addition, a significant wintertime trend in Nordic Sea cyclone intensity of 2.6 % per decade is accordant with the long-term trend in the local pressure difference.

The overall trend in the Fram Strait pressure difference has been noted and used earlier (Widell et al., 2003; Kwok, 2009). Kwok (2009) also noted that the trend is strongest for January through March. Throughout the year we found the correlations between the cyclones and the pressure trends to be weaker, but still there for autumn

TCD
5, 1311–1334, 2011

and spring. Direct observations from ships confirm the trend in the NCEP reanalysis mean sea level pressure over the North Atlantic (Chang, 2007). However, the trends in filtered mean sea level pressure variance statistics (mainly a measure of cyclone intensity) was about 70 % to 80 % of that found in the NCEP reanalysis, indicating that reanalysis trends may be influenced by density changes of the observational network.

A trend in Fram Strait sea ice area export has not been detected by most previous studies. Vinje (2001) found no visible trend for the period 1950–2000, but based on our relation between pressure difference and area export (Eq. 3) we get a trend of ∼3% per decade for the years 1957–2000. Kwok (2009) did also not find a trend for the period 1979–2007. Using our data we find a trend of ∼ 4% per decade for these years. Overall we find a robust trend for 1957–2010 with a magnitude of 5 % per decade, and similar trends onwards from 1970, 1980 and 1990. This indicates a gradually increasing ice export over the last 50 years. The trend is a direct change in boundary conditions to the Arctic sea ice. It is likely that the low export during the 1960's (Fig. 7) contributed directly to a thicker ice cover during that decade than for the long-term average Kwok and Rothrock (2009). The seemingly constant Arctic sea ice thickness during the 1990's (Winsor, 2001) is consistent with the low export between 1996 and 1999 (Fig. 7). Recent thinning and smaller sea ice cover reflects the increasing export onwards from 2003.

Prior to 2004, the reanalysis based (Fig. 7 and Eq. 3) time series does not carry any information of possible cross-strait changes in width, ice speed, or ice concentration. We did consider blending in the ice concentration data back to 1979 with the slightly higher correlation of the ice speed (Eq. 1). However, because our results for 1979–2004 are similar to Kwok (2009) we belive any cross-strait changes have minor importance for this period. For the period 1957–1979 only the re-analysis are available, and any estimates of ice area flux will have to be model based for this period.

TCD
5, 1311–1334, 2011

4.3 The SAR–AMSR differences

Figure 6 shows the winter AMSR data coverage since 2004. An estimate of the ice area export along 79° N based on these data would be highly dependent on interpolation, especially for the region where most of the ice export occurs. Our SAR based ice area export estimates shows larger annual values and variability than earlier estimates of ice export (Vinje, 2001; Widell et al., 2003; Kwok, 2009), which were based on east-west extrapolation between single moorings, or passive microwave satellite data. It is not the lack of data from the passive satellites during summer that creates the difference, our summer values (Fig. 3) are close to existing estimates (Kwok, 2009). The largest and most important ice export occurs during winter and in a longitudinal band that have previously not been adequately sampled.

The yearly cycle (Fig. 3) and periods with high and low ice export (Fig. 7) are consistent with earlier estimates (Kwok, 2009). We find a similar maximum for the sea ice export occurring in 1995, and low values in the late 80's and 90's. Because the SAR based ice speed coverage is much better for the area where most of the sea ice export occurs than the passive satellites, our estimates should be the most accurate available today. For the SAR based time series (Fig. 4) we are using the same observations of ice concentration as Kwok (2009), so differences in sea ice concentration can not explain the difference. The increasing trend of 5 % per decade is largely created by high values after 2003, when our SAR based estimates are consequently high. The long-term trend is therefore robust towards our values prior to 2004.

4.4 Implications for summer seaice extent

Year to year variability of the summer ice cover could be produced within the Arctic Ocean by winter growth, summer melt, or ridging, or by ice export at the boundary (Perovich et al., 2008; Kwok and Cunningham, 2010; Ogi et al., 2008, 2010). Figure 7 shows that the annual variability in ice export is ~0.1 mill km^2, about 20 % of the variability in summer sea ice area (~0.5 mill km^2) (Stroeve and Meier, 2010). For 2005–

TCD
5, 1311–1334, 2011

2008 the annual ice export was high for four consecutive years, with values above 0.9 mill km^2 each year. This is unique over the last 50 years, is consistent with recent large scale wind shifts (Ogi et al., 2010), and must have contributed to the recent low summer sea ice covers. The Arctic seasonal maximum sea ice cover occurs in late February or early March (Zwally and Gloersen, 2008). This suggests that the spring and summer (March–August) ice export should directly influence the following summer sea ice minimum (Kwok and Cunningham, 2010). We find support for such influence, and see potential for a seasonal prediction of the summer minimum using the spring export.

The summer export is normally less than half of that during the spring (Fig. 3). Previous to the historical minimum in 2007 the autumn and winter export stayed almost constant, but the spring and summer export doubled (2005: 0.183 mill km^2, 2006: 0.309 mill km^2 and 2007: 0.402 mill km^2). In 2008, when the summer minimum re-bounced, the spring and summer area export did not increase further (0.405 mill km^2). The last two years both annual (Fig. 7) as well as spring and summer export (2009: 0.381 mill km^2 and 2010: 0.321 mill km^2) ended up lower than 2007. A new record in September minima for 2009 and 2010 was thus not expected based on the sea ice export forcing.

5 Conclusions

We presented Fram strait southward ice velocity based on high accuracy Synthetic Aperture Radar (SAR) data onwards from 2004. Using available ice concentration data we found the mean yearly ice area export for 2004–2010 to be 0.888 mill km^2. This value is ~25 % higher than the 1979–2007 average from Kwok (2009). The high sea ice area export must have been a significant contributor to the low September sea ice covers observed in recent years. The sea ice area export in 2009 and 2010 was lower than for the previous years, 2005, 2006, 2007 and 2008, perhaps indicating that the sea ice export may return to more moderate levels again soon.

TCD
5, 1311–1334, 2011

High correlations between the ice drift and geostrophic winds from atmospheric reanalysis data allowed for calculations of the sea ice area export back to the 1950's. Our long term mean value (1957–2010) is 0.771 mill km^2, 10 % higher than the earlier estimate (Kwok, 2009). We found a robust trend for 1957–2010 with a magnitude of 5 % per decade, and similar trends onwards from 1970, 1980 and 1990. This indicates a gradually increasing ice export over the last 50 years, and is a direct change in boundary conditions to the Arctic sea ice. The positive trend is produced by a trend in the local pressure gradient, related to intensification of cyclones over the Nordic Seas.

The dramatic loss of Arctic sea ice the last decades is thus only partly caused by increased long-wave radiation related to ongoing atmospheric CO_2 increase (Smedsrud et al., 2008). A number of feedback effects have contributed once the ice thickness decreased (Perovich et al., 2008; Rampal et al., 2009; Screen and Simmonds, 2010), but as demonstrated by the General Circulation Models, additional forcing is needed to explain ongoing changes. Contrary to previous conclusions (Vinje, 2001; Kwok, 2009), the ice export has likely been an effective contributor to Arctic ice loss since the 1960's.

Acknowledgements. The reanalysis data were obtained from the National Center for Environmental Prediction (NCEP) data server, and the ERA-40 data from the European Centre for Medium-Range Weather Forecasts (ECMWF) data server. We would like to thank an anonymous reviewer for helpful suggestions, and Ron Kwok for supplying his ice export data. This work was supported by the NorClim, Pocahontas and Damocles projects, and is publication A327 from the Bjerknes Centre for Climate Research.

TCD
5, 1311–1334, 2011

References

Anderson, D., Hodges, K. I., and Hoskins, B. J.: Sensitivity of feature-based analysis methods of storm tracks to the form of background field removal, Mon. Wea. Rev., 131, 565–573, 2003. 1315

Björk, G.: The relation between ice deformation, oceanic heat flux, and the ice thickness distribution in the Arctic Ocean, J. Geophys. Res., 102, 18689–18698, 1997. 1313

Boe, J., Hall, A., and Qu, X.: September sea-ice cover in the Arctic Ocean projected to vanish by 2100, Nat. Geosci., 2, doi:10.1038/NGEO467, 2009. 1313

Chang, E. K. M.: Assessing the increasing trend in Northern Hemisphere winter storm track activity using surface ship observations and a statistical storm track model, J. Climate, 20, 5607–5628, doi:10.1175/2007jcli1596.1, 2007. 1321

Ezraty, R., Girard-Ardhuin, F., and Croiz-Fillon, D.: Sea ice drift in the central Arctic using the 89 GHz brightness temperatures of the Advanced Microwave Scanning Radiometer, http://www.ifremer.fr/cersat, 2010. 1317

Foldvik, A., Aagaard, K., and Tørresen, T.: On the velocity field of the East Greenland Current, Deep-Sea Res, 35, 1335–1354, 1988. 1317

Gloersen, P. and Campbell, W. J.: Recent variation in Arctic and Antarctic sea-ice covers, Nature, 352, 33–36, 1991. 1312

Haas, C., Pfaffling, A., Hendricks, A. S., Rabenstein, L., Etienne, J. L., and Rigor, I.: Reduced ice thickness in Arctic Transpolar Drift favors rapid ice retreat, Geophys. Res. Lett., 35, doi:10.1029/2000JC000723, 2008. 1313

Hakkinen, S., Proshutinsky, A., and Ashik, I.: Sea ice drift in the Arctic since 1950s, Geophys. Res. Lett., 35, doi:10.1029/2008GL034791, 2008. 1313, 1319, 1320

Hodges, K. I.: A general method for tracking analysis and its application to meteorological data, Mon. Wea. Rev., 122, 2573–2586, 1994. 1315

Hodges, K. I.: Adaptive constraints for feature tracking, Mon. Wea. Rev., 127, 1362–1373, 1999. 1315

Kalnay, E., Kanamitsu, M., Kistler, R., Collins, W., Deaven, D., Gandin, L., Iredell, M., Saha, S., White, G., Woollen, J., Zhu, Y., Chelliah, M., Ebisuzaki, W., Higgins, W., Janowiak, J., Mo, K. C., Ropelewski, C., Wang, J., Leetmaa, A., Reynolds, R., Jenne, R., and Joseph, D.: The NCEP/NCAR 40-year reanalysis project, B. Am. Meteorol. Soc., 77, 437–471, 1996. 1314

Kloster, K. and Sandven, S.: Ice Motion and Ice Area Flux in Fram Strait at 79N using ASAR

TCD
5, 1311–1334, 2011

and passive microwave for Feb. 2004 – Jul. 2010, Tech. Rep. 322, Nansen Environmental and Remote Sensing Centre, Bergen, Norway, 2011. 1314
Kwok, R.: Outflow of Arctic Ocean sea ice into the Greenland and Barents Seas: 1979–2007, J. Climate, 22, 2438–2457, doi:10.1175/2008JCLI2819.1, 2009. 1313, 1314, 1317, 1319, 1320, 1321, 1322, 1323, 1324
Kwok, R. and Cunningham, C. F.: Contribution of melt in the Beaufort Sea to the decline in Arctic multiyear sea ice coverage: 1993–2009, Geophys. Res. Lett., 37, doi:10.1029/2010gl044678, 2010. 1322, 1323
Kwok, R. and Rothrock, D. A.: Decline in Arctic sea ice thickness from submarine and ICESat records: 1958–2008, Geophys. Res. Lett., 2009. 1321
Kwok, R., Cunningham, G., and Pang, S.: Fram Strait sea ice outflow, J. Geophys. Res., 109, C01009, doi:10.1029/2003JC001785, 2004. 1313, 1315
Nansen, F.: The Norwegian North Polar Expedition 1893–1896, Scientific Results, The Fridtjof Nansen fund for the advancement of science, 1–22, 1906. 1313
Ogi, M., Rigor, I. G., McPhee, M. G., and Wallace, J. M.: Summer retreat of Arctic sea ice: Role of summer winds, Geophys. Res. Lett., 35, doi:10.1029/2008gl035672, 2008. 1322
Ogi, M., Yamazaki, K., and Wallace, J. M.: Influence of winter and summer surface wind anomalies on summer Arctic sea ice extent, Geophys. Res. Lett., 37, doi:10.1029/2009gl042356, 2010. 1322, 1323
Overland, J., Wang, M., and Salo, S.: The recent Arctic warm period, Tellus, 60A, 589–597, doi:10.1111/j.1600-0870.2008.00327.x, 2008. 1313
Perovich, D. K., Richter-Menge, J. A., Jones, K. F., and Light, B.: Sunlight, water and ice: Extreme Arctic sea ice melt during the summer of 2007, Geophys. Res. Lett., 35, doi:10.1029/2008GL034007, 2008. 1313, 1322, 1324
Quenouille, M. H.: Associated Measurements, 242 pp, Butterworths Scientific, 1952. 1315
Rampal, P., Weiss, J., and Marsan, D.: Positive trend in the mean speed and deformation rate of Arctic sea ice, J. Geophys. Res., doi:10.1029/2008jc005066, 2009. 1314, 1319, 1324
Screen, J. A. and Simmonds, I.: The central role of diminishing sea ice in recent Arctic temperature amplification, Nature, 464, 1334–1337, 2010. 1313, 1324
Smedsrud, L. H., Sorteberg, A., and Kloster, K.: Recent and future changes of the Arctic Sea Ice Cover, Geophys. Res. Lett., 35, doi:10.1029/2008GL034813, 2008. 1313, 1324
Sorteberg, A. and Kvingedal, B.: Atmospheric Forcing on the Barents Sea Winter Ice Extent, J. Climate, 19, 4772–4784, 2006. 1315

TCD
5, 1311–1334, 2011

Sorteberg, A. and Walsh, J. E.: Seasonal cyclone variability at 70 degrees N and its impact on moisture transport into the Arctic, Tellus, 60, 570–586, doi:10.1111/j.1600-0870.2008.00314.x, 2008. 1315, 1320

Sorteberg, A., Kattsov, V., Walsh, J., and Pavlova, T.: The Arctic surface enrgy budget as simulated with the IPCC AR4 AOGCMs, Clim. Dynam., 29, 131–156, doi:10.1007/s00382-006-0222-9, 2007. 1313, 1315

Stroeve, J. and Meier, W.: Sea Ice Trends and Climatologies from SMMR and SSM/I, http://nsidc.org/data/seaice/data_summaries.html, 2010. 1312, 1322

Stroeve, J., Holland, M., Meier, W., Scambos, T., and Serreze, M.: Arctic sea ice decline: Faster than forecast, Geophys. Res. Lett., 34, doi:10.1029/2007GL029703, 2007. 1312, 1313

Thorndike, A. and Colony, R.: Sea Ice Motion in Response to Geostrophic Winds, J. Geophys. Res., 87, 5845–5852, 1982. 1315, 1316

Tsukernik, M., Deser, C., Alexander, M., and Tomas, R.: Atmospheric forcing of Fram Strait sea ice export: a closer look, Clim. Dynam., doi:10.1007/s00382-009-0647-z, 2009. 1315

Uppala, S. M., Kallberg, P. W., Simmons, A. J., Andrae, U., Bechtold, V. D., Fiorino, M., Gibson, J. K., Haseler, J., Hernandez, A. Kelly, G. A., Li, X., Onogi, K. Saarinen, S., Sokka, N., Allan, R. P., Andersson, E., Arpe, K., Balmaseda, M. A. Beljaars, A. C. M., Van De Berg, L., Bidlot, J., Bormann, N., Caires, S., Chevallier, F., Dethof, A., Dragosavac, M., Fisher, M., Fuentes, M., Hagemann, S., Holm, E., Hoskins, B. J., Isaksen, L. Janssen, P. A. E. M., Jenne, R., McNally, A. P., Mahfouf, J. F., Morcrette, J. J., Rayner, N. A., Saunders, R. W., Simon, P., Sterl, A., Trenberth, K. E., Untch, A., Vasiljevic, D., Viterbo, P., and Woollen, J.: The ERA-40anett re-analysis, Q. J. Roy. Meteorol. Soc., 131, 2961–3012, 2005. 1316, 1320

Vinje, T.: Fram strait ice fluxes and atmospheric circulation: 1950–2000, J. Climate, 14, 3508–3517, 2001. 1313, 1315, 1320, 1321, 1322, 1324

Widell, K., Østerhus, S., and Gammelsrød, T.: Sea ice velocity in the Fram Strait monitored by moored instruments, Geophys. Res. Lett., 30(19), 1982, doi:10.1029/2003GL018119, 2003. 1315, 1317, 1320, 1322

Winsor, P.: Arctic Sea Ice Thickness Remained Constant During the 1990s, Geophys. Res. Lett., 28, 1039–1041, 2001. 1321

Zwally, H. J. and Gloersen, P.: Arctic sea ice surviving the summer melt: interannual variability and decreasing trend, J. Glaciol., 54, 279–296, 2008. 1312, 1323

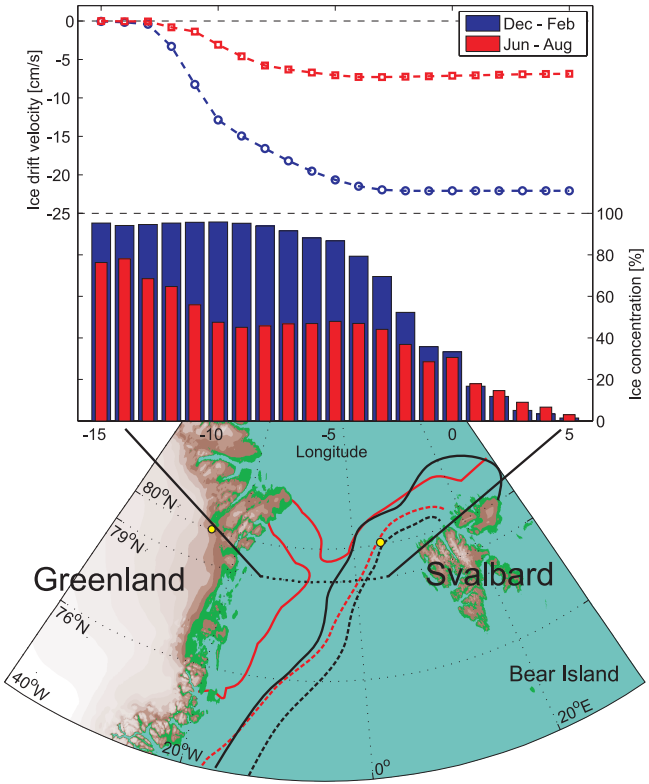

Fig. 1. The Fram Strait between Greenland and Svalbard and mean sea ice properties for 2004–2010. Ice cover for summer (red, June through August) and winter (black, December through February) as solid (50 %) and dashed lines (15 %) . Above: southward ice drift across 79° N from August 2004 to July 2010 in 1° bins based on SAR imagery, and ice concentration from SSMI and AMSR data. The ice area export is found by multiplying the ice drift and ice concentrations. Yellow circles show locations for surface pressure data used.

TCD
5, 1311–1334, 2011

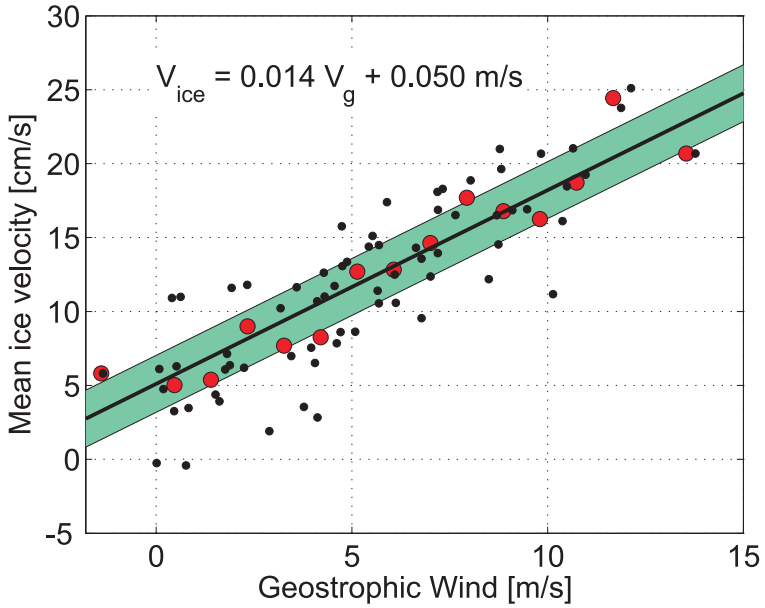

Fig. 2. Linear fit between Fram Strait southward ice velocity and geostrophic wind. Monthly averages are shown as black dots and are averaged along 79° N. Binned values are shown as red circles. The shaded area is the standard error estimate of the linear fit.

TCD
5, 1311–1334, 2011

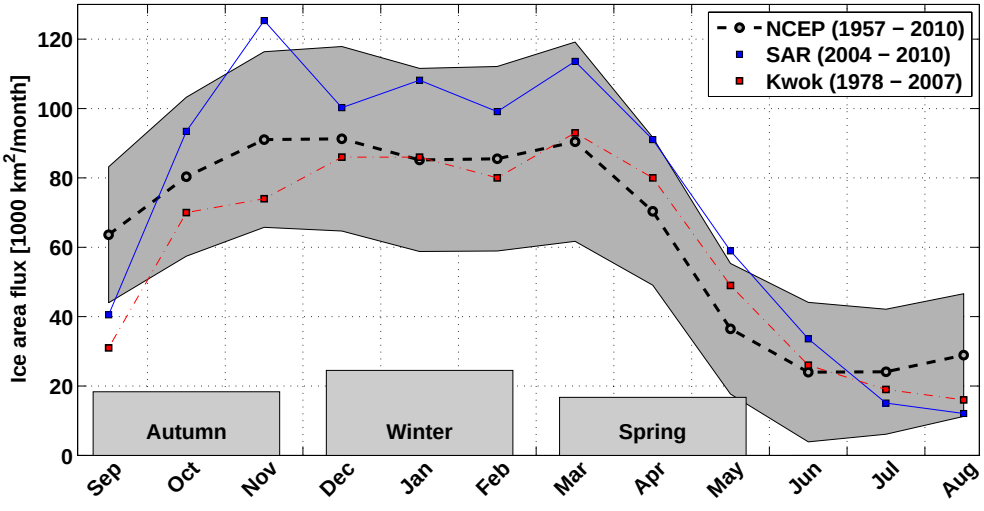

Fig. 3. Monthly mean Fram Strait sea ice area export during the year. Values from Kwok (2009) are added for comparison. Standard deviations of the NCEP values are shaded in grey. Changes in seasonal monthly ice export (1957–2010) are plotted at the bottom.

TCD
5, 1311–1334, 2011

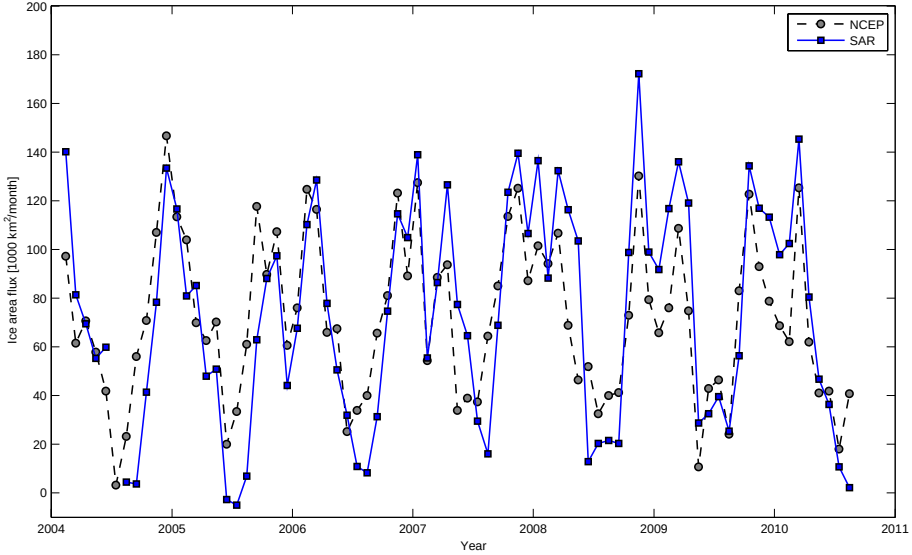

Fig. 4. Monthly ice area export values based on SAR velocity compared to the NCEP pressure difference formula (Eq. 3.)

TCD
5, 1311–1334, 2011

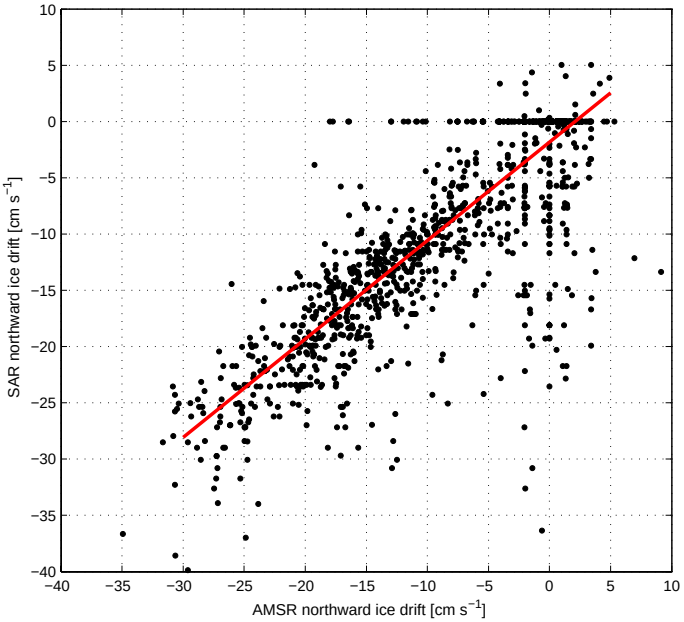

Fig. 5. Comparison between southward ice drift speeds across 79° N in the Fram Strait from SAR and AMSR data. The data covers winters (October through April) between 2004 and 2010. Individual values are estimated 3-days drift velocities for a given longitude bin. Red line is a linear fit.

TCD
5, 1311–1334, 2011

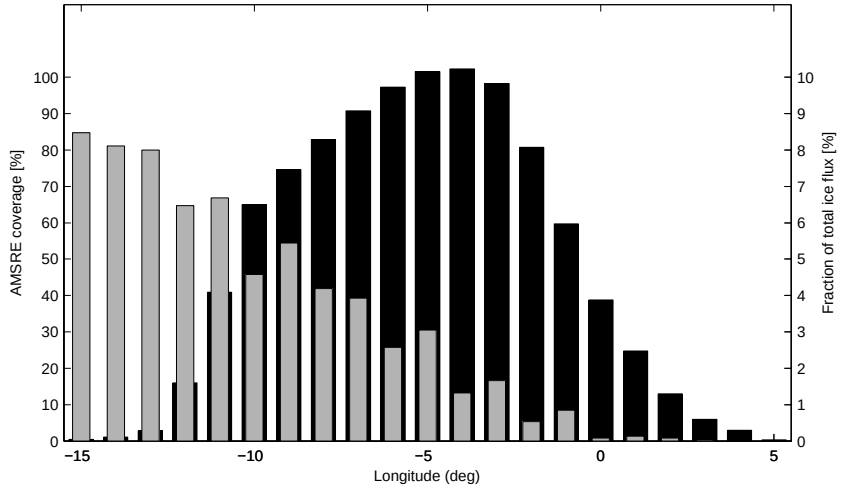

Fig. 6. Coverage of AMSR ice speed data along 79° N in the Fram Strait, contrasted with our new SAR based ice area export estimates. The period covered is October through April from 2004 to 2010. A 50 % value (grey bars, left axis) means that the actual longitude bin has AMSR ice drift velocity estimates for 50 % of the time. Black bars shows the contribution to the total ice flux for the individual longitude bins (right axis), calculated from the SAR ice drift velocities for the same period. The SAR data coverage is 100% for all bins, i.e. we have an ice velocity measurement for every bin every 3 days.

TCD
5, 1311–1334, 2011

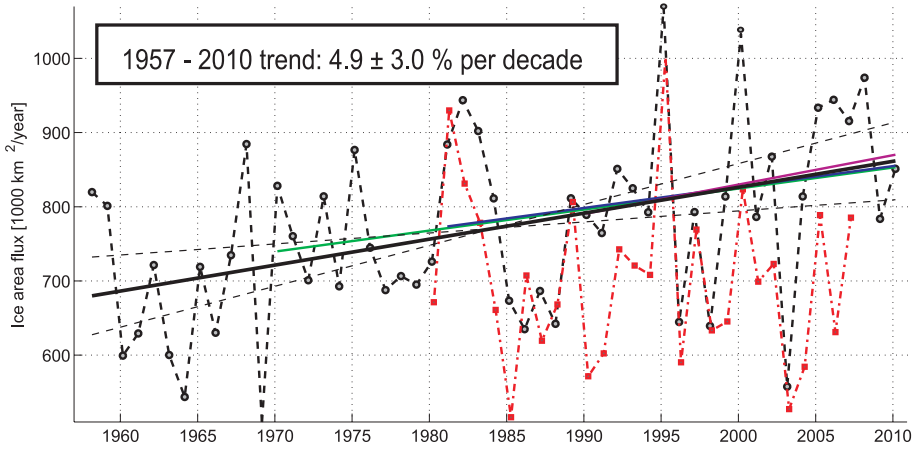

Fig. 7. Annual mean Fram Strait sea ice area export values as driven by NCEP surface pressure difference. Values are averages for 1 September through 31 August. Dashed lines indicate the 95 % confidence interval of the trend. Linear trends are added onwards from 1970, 1980 and 1990 (different colours). Values from Kwok (2009) are added for comparison.

TCD
5, 1311–1334, 2011